

# Thermalization from quenching in coupled oscillators

M Harinarayanan<sup>1,\*</sup> and Karthik Rajeev<sup>2,†</sup>

<sup>1</sup>*Bharata Mata College, Thrikkakara, Kochi 682021, Kerala, India*

<sup>2</sup>*Higgs Centre, School of Physics and Astronomy, University of Edinburgh, EH9 3FD, UK*

We introduce a finite-time protocol that thermalizes a quantum harmonic oscillator, initially in its ground state, without requiring a macroscopic bath. The method uses a second oscillator as an effective environment and implements sudden quenches of the oscillator frequencies and coupling. Owing to the Gaussian nature of the dynamics, the thermalization condition reduces to three solvable equations, yielding exact analytic solutions for a dense discrete set of temperatures and numerical solutions in all other cases. Any target temperature can be approximated with arbitrary precision, with a trade-off between speed and accuracy. The simplicity of the protocol makes it a promising tool for rapid, controlled thermalization in quantum thermodynamics experiments and state preparation.

## I. INTRODUCTION

The concept of thermalization is central to both classical and quantum physics, underpinning the emergence of equilibrium properties from microscopic dynamics. Thermality also remains a key topic in contemporary research across quantum information[1, 2], many-body physics[3], and even quantum gravity[4, 5].

Addressing this aspect for quantum systems is the focus of the rapidly growing field of quantum thermodynamics (for recent reviews, see [6, 7]). In addition to its fundamental significance, advancing our understanding of quantum thermodynamic processes is expected to play an important role in the development of future technologies, particularly at the nanoscale[8, 9], where quantum effects become dominant. In quantum simulations[10]—positioned at the intersection of advanced technology and fundamental physics—efficient preparation of thermal states plays a crucial role in multiple applications. Therefore, there are both theoretical and experimental efforts to improve and optimize the preparation of thermal states of quantum systems[11, 12].

The quantum harmonic oscillator (QHO) is not only a fundamental exactly solvable model in quantum mechanics but also a key component of various physical platforms—from vibrational modes in trapped ions to superconducting resonators in circuit QED, as well as optomechanical mirrors and nanomechanical membranes [13–16]. Consequently, the QHO holds a central role in the study of thermodynamics of quantum systems[17–20].

Traditionally, thermalization of a quantum harmonic oscillator (QHO) is achieved by coupling it

to a heat bath and allowing equilibration over long timescales. Recent works have extended this framework to finite baths [21–23] and developed formulations that treat the bath and system on equal footing [24]. In parallel, advances in nonequilibrium quantum control have motivated alternative approaches, including engineered *shortcuts* to inherently slow processes such as adiabatic evolution [25, 26].

Building on these ideas, our work proposes a protocol that achieves *exact* thermalization of QHO within a *finite time* by substituting the conventional heat bath with a second *identical* QHO and time-dependent control. Thermalization is driven by a sequence of sudden quenches applied to the frequencies and couplings of the two-oscillator system, effectively preparing the target thermal state without the need for long interactions with a macroscopic reservoir.

The paper is structured as follows: We begin by briefly reviewing relevant aspects of pure Gaussian states of a system of two bosonic oscillators, and setting up notations and conventions in [Section II](#). Following that, in [Section III](#), we introduce the general set-up on which our prescription is based. In [Section IV](#), we outline the main result of this paper, namely, the prescription to achieve thermalization of a bosonic oscillator in *finite time* using our setup. Finally, we conclude with a summary and future outlook in [Section V](#). ( $\hbar = k_B = 1$ , unless otherwise stated.)

## II. REVIEW OF TWO-MODE GAUSSIAN PURE STATES

The core idea behind the thermal state preparation method proposed in this work relies on the properties of Gaussian pure states associated with a two-oscillator system. To set the stage, we begin with a

\* [mharinarayanan7@gmail.com](mailto:mharinarayanan7@gmail.com)

† [karthik.rajeev@ed.ac.uk](mailto:karthik.rajeev@ed.ac.uk)

brief review of the essential concepts and establish the notation that will be used throughout the rest of the paper.

We label the two oscillators as *oscillator-1* (the system) and *oscillator-2* (the environment), with coordinates  $x_1$  and  $x_2$ , respectively. For simplicity of the discussion, the oscillators have identical mass  $m$  and frequency  $\omega$ . A general *undisplaced* Gaussian pure state of the combined system can be described by the wavefunction:

$$\psi(x_1, x_2) = \mathcal{N} \exp \left[ - \sum_{i,j=1}^2 \frac{A_{ij}}{2} x_i x_j \right], \quad (1)$$

where  $\mathcal{N}$  is the normalization factor and the complex coefficients  $A_{ij}$  satisfy  $\text{Re}[A_{11}], \text{Re}[A_{22}] > 0$  and  $2\text{Re}[A_{11}]\text{Re}[A_{22}] > \text{Re}[A_{12}^2]$ .

Since *oscillator-1* is the system we want to do manipulations on, we shall be interested in the reduced density matrix  $\rho_{x'_1 x'_1}^{(1)}$  of the same, obtained by tracing over  $x_2$  and which takes the form:

$$\begin{aligned} \rho_{x'_1 x'_1}^{(1)} &= |\mathcal{N}|^2 \int_{-\infty}^{\infty} \psi^*(x'_1, x_2) \psi(x_1, x_2) dx_2, \quad (2) \\ &= |\mathcal{N}|^2 e^{-\frac{m\omega}{2} [(X+iY)x'_1{}^2 + (X-iY)x_1^2 + 2Zx'_1 x_1]}. \end{aligned}$$

Here, the real dimensionless parameters  $X, Y$  and  $Z$  are defined by

$$X + iY = \frac{1}{m\omega} \left( A_{11} - \frac{A_{12}^2}{2\text{Re}[A_{22}]} \right), \quad (3)$$

$$Z = -\frac{1}{m\omega} \left( \frac{|A_{12}|^2}{2\text{Re}[A_{22}]} \right). \quad (4)$$

These parameters are, of course, related to the components of the covariance matrix through

$$\begin{bmatrix} \Sigma_{xx} & \Sigma_{xp} \\ \Sigma_{px} & \Sigma_{pp} \end{bmatrix} = \frac{1}{2} \begin{bmatrix} \frac{1}{X+Z} & \frac{i(X+iY+Z)}{X+Z} \\ \frac{-i(X-iY+Z)}{X+Z} & \frac{X^2+Y^2-Z^2}{X+Z} \end{bmatrix}. \quad (5)$$

The reduced density matrix is therefore equally fully characterized by the real variables  $X, Y$  and  $Z$ . Since we are interested in dynamical density matrices, these parameters vary with time, allowing the evolution of the density matrix to be conveniently represented by the three-dimensional curve

$$\vec{R}(t) \equiv (X(t), Y(t), Z(t)). \quad (6)$$

The main goal of this paper is to prescribe a method to dynamically generate a thermal state, for which the density matrix  $\rho_\beta$  takes the form

$$\langle x_1 | \rho_\beta | x'_1 \rangle \propto e^{-\frac{m\omega}{2} [(x_1^2 + x'_1{}^2) \coth \beta \omega - 2x_1 x'_1 \text{csch}(\beta \omega)]}, \quad (7)$$

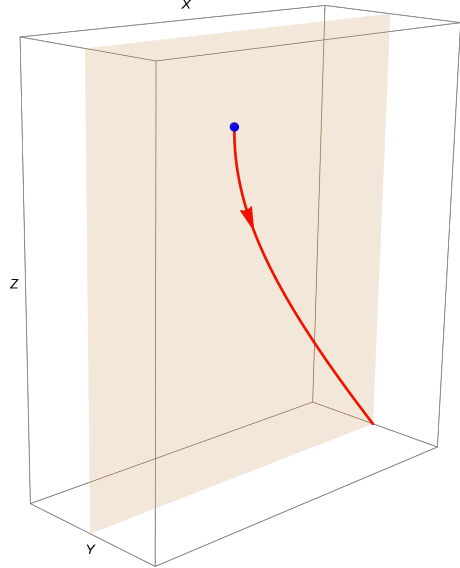


**FIG. 1:** The family of thermal density matrices is represented by the curve  $\vec{R}_\beta = (\coth(\beta\omega), 0, -\text{cosech}(\beta\omega))$ . The curve lies entirely in the  $X$ - $Z$  plane, shown as the shaded region, where it is described by part of the hyperbola  $Z = -\sqrt{X^2 - 1}$ . The blue dot indicates the ground state, and the arrow shows the direction of increasing temperature.

where  $\beta = 1/T$  is the inverse temperature. This translates to

$$\vec{R} \rightarrow \vec{R}_\beta \equiv (\coth(\beta\omega), 0, -\text{cosech}(\beta\omega)), \quad (8)$$

which describes a one-parameter curve in the  $\vec{R}$ -space as shown in Fig. 1. Since the above equations impose three distinct constraints, it is natural to expect that a suitably designed Hamiltonian evolution for the coupled oscillators—with three tunable parameters—could dynamically produce a desired thermal state, given appropriate adjustments of those parameters. In the following section, we demonstrate that this is indeed achievable through a concrete example.

### III. THE SET UP

We consider a system of two coupled oscillators described by a Hamiltonian of the form:

$$\begin{aligned} H = & \frac{1}{2m} p_1^2 + \frac{1}{2m} p_2^2 + \frac{1}{2} m\Omega^2(t)x_1^2 + \frac{1}{2} m\Omega^2(t)x_2^2 \\ & + \frac{1}{2} \mathcal{K}(t)(x_1 - x_2)^2, \end{aligned} \quad (9)$$

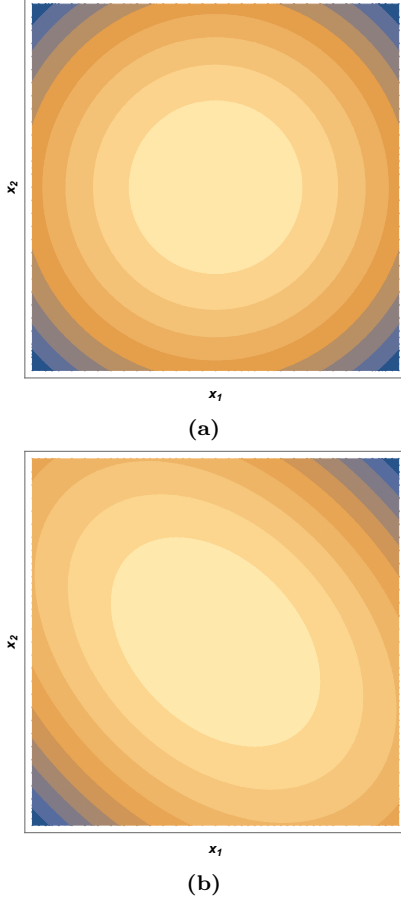


**FIG. 2:** Contour representation of the effective 2D potential of the coupled oscillator system, for typical values of  $\omega'/\omega$  and  $k/\omega^2$ , when the system is in (a) the uncoupled phase, and (b) the coupled phase ( $0 < t < \tau$ ).

where we shall refer to  $\mathcal{K}$  as the ‘coupling’. Henceforth, without loss of generality, we shall set  $m = 1$ . The above Hamiltonian can also be interpreted as describing a particle confined in a time-dependent two-dimensional harmonic potential well. For our proposal, we assume the following time dependence for the frequency and coupling:

$$\begin{aligned} \mathcal{K}(t) &= \begin{cases} k & ; \quad 0 < t < \tau \\ 0 & ; \quad \text{otherwise} \end{cases}, & (10) \\ \Omega(t) &= \begin{cases} \omega & ; \quad t < 0 \text{ and } t > \tau \\ \omega' & ; \quad 0 < t < \tau \end{cases}, \end{aligned}$$

where,  $k$ ,  $\omega'$  and  $\tau$  are tuneable. The time dependence of the potential, when realised in the context of trapped ions(such as in [13]), can then be visualized as a kind of squeezing of the equipotential

contours as shown in [Fig. 2](#).

The quantum dynamics of time-dependent coupled oscillators is well understood. In the special case of Gaussian pure states, the dynamics can be fully described in terms of solutions to the classical equations of motion of the normal modes. In terms of the normal modes—which are  $x_{\pm} = (x_1 \pm x_2)/\sqrt{2}$ , with normal mode frequencies  $\Omega_{+}(t) = \Omega(t)$  and  $\Omega_{-}(t) = \sqrt{\Omega^2(t) + 2\mathcal{K}(t)}$ —the problem reduces to that of two time dependent uncoupled oscillators. This standard procedure leads to a Gaussian wavefunction of the form in [Eq. \(1\)](#), with  $A_{ij}$  being functions of time. Specifically,

$$A_{11}(t) = A_{22}(t) = \sum_{\sigma=+,-} \left( \frac{\Omega_{\sigma}(0)}{2b_{\sigma}^2} - \frac{i\dot{b}_{\sigma}}{2b_{\sigma}} \right), \quad (11)$$

$$A_{12}(t) = \sum_{\sigma=+,-} \sigma \left( \frac{\Omega_{\sigma}(0)}{2b_{\sigma}^2} - \frac{i\dot{b}_{\sigma}}{2b_{\sigma}} \right), \quad (12)$$

where, the functions  $b_{\pm}(t)$  satisfy

$$\ddot{b}_{\pm} + \Omega_{\pm}^2(t)b_{\pm} = \frac{\Omega_{\pm}^2(0)}{b_{\pm}^3}. \quad (13)$$

The above *non-linear* equations are nothing but the Ermakov equations [27–29] corresponding to the normal modes.

We now focus on the specific quench-type time dependence defined in [Equation Eq. \(10\)](#), for which  $\Omega_{+}(0) = \omega'$  and  $\Omega_{-}(0) = \sqrt{\omega'^2 + 2k}$ . We demand that the full system is initialized in the ground state at  $t = 0$ , when the system is uncoupled. This translates to the initial conditions of the form  $b_{\pm}(0) = 1$ , and  $\dot{b}_{\pm} = 0$ . The exact solutions in this case, for  $0 < t < \tau$ , turns out to be:

$$b_{+}(t) = \sqrt{\frac{\omega^2 \sin^2(\omega' t)}{\omega'^2} + \cos^2(\omega' t)}, \quad (14)$$

$$b_{-}(t) = \sqrt{\frac{\omega^2 \sin^2(\eta\omega' t)}{\eta^2\omega'^2} + \cos^2(\eta\omega' t)}, \quad (15)$$

where,  $\eta^2 \equiv \frac{\omega'^2 + 2k}{\omega'^2}$ . In summary, the full quantum dynamics of the system, when prepared in the ground state at  $t = 0$ , is contained in [Eq. \(14\)](#) and [Eq. \(15\)](#).

To visualize the evolution of the density matrix that follows from the above solutions, we can derive the corresponding  $\tilde{R}(t)$  that follows from [Eq. \(3\)](#) and [Eq. \(11\)](#)–[Eq. \(15\)](#). For arbitrary values of the tuneable parameters  $\omega'$ ,  $k$ , and  $\tau$ , the resulting evolution does not necessarily lead to the thermal state. To demonstrate this visually, in [Fig. 3](#) we present the

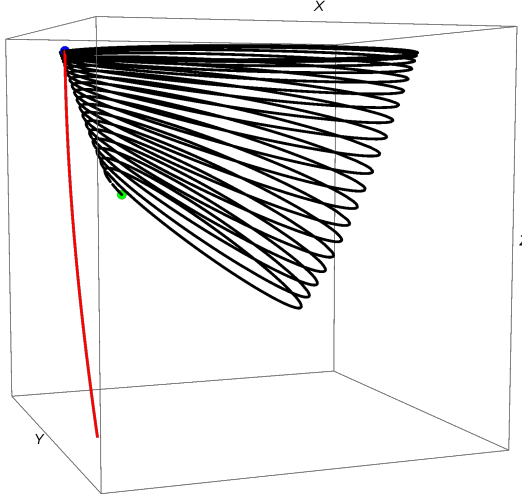


**FIG. 3:** Evolution of  $\rho_{x_1 x'_1}^{(1)}$  represented in the  $\vec{R}$ -space, assuming a randomly chosen set of the tunable parameters  $\omega'$ ,  $k$  and  $\tau$ . The *oscillator-1* is initially in the ground state (blue dot) and evolves, at  $t = \tau$ , to the green point. The red curve is the family of thermal states.

evolution of  $\vec{R}(t)$  for a random choice of these parameters. Note again that the red curve represents the family of thermal states, and clearly, the density matrix does not evolve to this line in this specific example. In the next section, we shall show that by tuning the above parameters, we can prepare the reduced density matrix of one of the oscillators in a thermal form.

#### IV. THERMALIZATION FROM QUENCHING

We begin with a brief schematic overview, as illustrated in [Fig. 4](#), demonstrating how our framework enables the preparation of *oscillator-1* in its thermal state. Recall that *oscillator-1* is the system of interest and is initially prepared in its ground state. The method also involves a second, identical oscillator (*oscillator-2*), which is likewise initialized in the ground state and decoupled from *oscillator-1* initially. In the trapped-ion implementation of this setup, such ground-state preparation can be achieved, for example, via laser cooling, as in [\[30, 31\]](#).

To rephrase the time dependence of the system as described by [Eq. \(10\)](#) in more physical terms, define an *active-phase* during which the coupling of strength  $k$  is suddenly switched on between the two

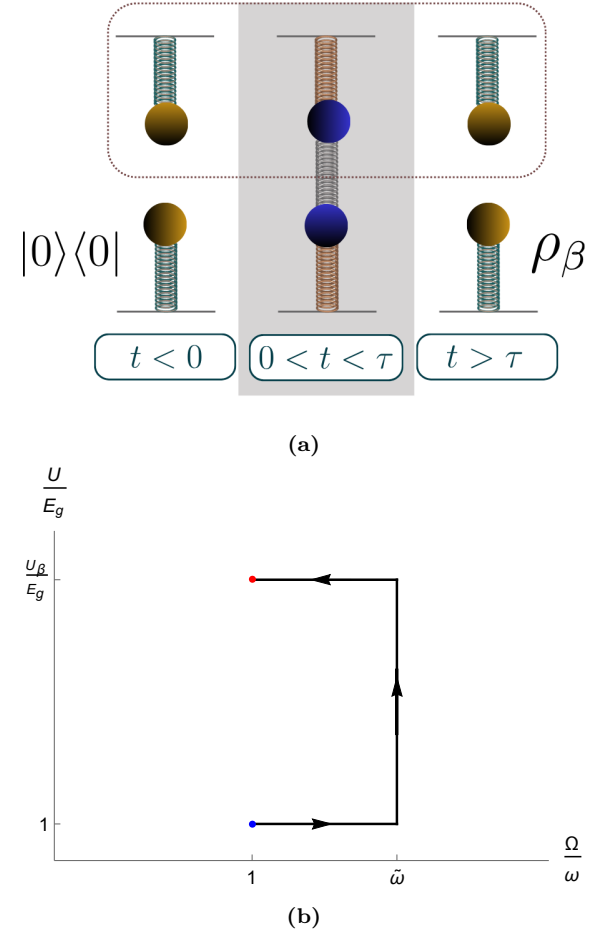


**FIG. 4:** (a) Protocol for preparing *oscillator-1* in a thermal state. Both oscillators start in their ground states and are initially decoupled. A coupling of strength  $k$  is suddenly introduced, and their frequencies are shifted to  $\omega'$  for a duration  $\tau$  (the *active-phase*). The oscillators are then decoupled and their frequencies reset to  $\omega$ . Tuning  $k$ ,  $\omega'$ , and  $\tau$  brings *oscillator-1* to a thermal state at  $t = \tau$ . (b) The energy-frequency diagram for *oscillator-1* as it undergoes the protocol.

oscillators, and their frequencies are abruptly shifted to a new value  $\omega'$ . This phase lasts for a duration  $\tau$ , after which the oscillators are decoupled and their frequencies are restored to the original value  $\omega$ , marking the end of the *active-phase*. We will now show that, by suitably tuning  $k$ ,  $\omega'$ , and  $\tau$ , *oscillator-1* evolves into a thermal state at time  $t = \tau$ . To this end, it is convenient to introduce the following dimensionless parameters:

$$\tilde{\omega}' \equiv \frac{\omega'}{\omega}, \quad \tilde{k} \equiv \frac{k}{\omega^2}, \quad \tilde{\tau} \equiv \frac{\omega\tau}{2\pi}, \quad (16)$$

which allows us to express the tunable quantities in terms of  $\omega^{-1}$ , which is the natural time scale of the oscillators in the uncoupled state.

In the previous section, we outlined how the reduced density matrix  $\rho_{x_1 x'_1}^{(1)}$  of *oscillator-1* evolves in our setup, showing that its dynamics can be effectively captured by the vector  $\vec{R}(t)$ . Therefore, the condition that *oscillator-1* thermalizes at  $t = \tau$  can be written concisely as

$$\vec{R}(\tau) = \vec{R}_\beta. \quad (17)$$

In term of the solutions  $b_\pm(t)$  of the Ermakov equations [Eq. \(13\)](#), the above condition gives rise a system of three algebraic equations for the unknowns  $k$ ,  $\tilde{\omega}'$ , and  $\tilde{\tau}$ . The goal, then, is to solve the system for a given temperature  $T = 1/\beta$ , in order to determine the appropriate values of  $\tilde{k}$ ,  $\tilde{\omega}'$ , and  $\tilde{\tau}$  that correspond to that temperature.

Although this system of equations does not appear to yield an exact analytical solution for arbitrary temperatures, it is, in principle, amenable to numerical solution, thereby confirming the theoretical feasibility of our protocol. Interestingly, however, we will now examine a *special discrete set* of temperature values — dense in the positive real line — for which the otherwise complicated system does admit exact analytical solutions.

### A. Special discrete set of thermal states

The classical dynamics of coupled oscillators display quasi-periodicity due to the presence of two normal modes frequencies, which are generally incommensurate. This characteristic persists in the quantum dynamics as well, as reflected in our setup by the forms of the solutions  $b_\pm(t)$  in [Eq. \(14\)](#) and [Eq. \(15\)](#). However, in the special case where the normal modes are commensurate, the system becomes periodic. By inspection, we found that in this periodic limit the system of equations [Eq. \(17\)](#), which determines the value of tunable parameters for achieving thermalization, admits an exact analytical solution for a *special discrete set*(SDS) of temperatures, as we shall now demonstrate.

The condition of periodicity, during the *active-phase*, means that  $\tilde{\omega}'/\sqrt{\tilde{\omega}'^2 + 2\tilde{k}}$  is a rational number. Of special interest to us is the case where this ratio takes the form of an odd-over-odd fraction, i.e.,  $p/q$  where  $p$  and  $q$  are odd integers. Under these as-

sumptions, we propose the choice

$$\tilde{\tau} = \frac{1}{4\tilde{\omega}'}(2l + 1) = \frac{1}{4\sqrt{\tilde{\omega}'^2 + 2\tilde{k}}}(2n + 1), \quad (18)$$

where  $l, n \in \mathbb{W}$ . Physically, the first condition requires tuning  $\tau$  to an odd multiple of one-quarter of the period associated with the normal mode  $x_+$ . The second line then *follows* under our assumption that  $\tilde{\omega}'/\sqrt{\tilde{\omega}'^2 + 2\tilde{k}}$  is an odd-over-odd fraction. The motivation behind our assumptions till [Eq. \(18\)](#) is that one of the conditions in [Eq. \(17\)](#)—namely,  $Y(\tau) = 0$ —is then automatically satisfied.

To solve the rest of the equations, let us denote by  $\eta$  the ratio of the normal mode frequencies in the *active phase*:

$$\eta = \frac{\sqrt{\tilde{\omega}'^2 + 2\tilde{k}}}{\tilde{\omega}'} = \frac{2n + 1}{2l + 1} \quad (19)$$

where the second line follows from [Eq. \(18\)](#). The thermalization condition, under the aforementioned assumptions, then reduces to

$$\frac{(\eta^4 + 6\eta^2 + 1)}{(\eta^2 - 1)^2} = \cosh(\omega\beta) \quad (20)$$

$$\frac{4(\eta^2 + 1)}{\tilde{\omega}'^2(\eta^2 - 1)^2} = \sinh(\omega\beta) \quad (21)$$

It is easy to show that the above equations are solved by:

$$\frac{1}{\tilde{\omega}'^2} = \eta = \left[ \tanh\left(\frac{\beta\omega}{4}\right) \right]^{\pm 1} = \frac{2n + 1}{2l + 1}. \quad (22)$$

Further solving for  $\tilde{\omega}'$  and  $\tilde{k}$  explicitly, we arrive at the final result:

$$\frac{E_g}{k_B T_{nl}} \equiv \begin{cases} 2 \tanh^{-1}\left(\frac{2l+1}{2n+1}\right) & ; l < n \\ 2 \coth^{-1}\left(\frac{2l+1}{2n+1}\right) & ; l > n \end{cases}, \quad (23)$$

$$= \log\left(\frac{n+l+1}{|n-l|}\right)$$

$$\tilde{\omega}' = \sqrt{\frac{2l+1}{2n+1}} \equiv \tilde{\omega}'_{nl}, \quad (24)$$

$$\tilde{k} = \frac{2(n-l)(n+l+1)}{(2l+1)(2n+1)} \equiv \tilde{k}_{nl}, \quad (25)$$

$$\tilde{\tau} = \frac{1}{4} \sqrt{(2l+1)(2n+1)} \equiv \tilde{\tau}_{nl}, \quad (26)$$

where  $T_{nl}$  denotes the temperature and the last line is obtained by substituting the solutions of  $(\tilde{\omega}', \tilde{k})$

into Eq. (18). Note that we have retained  $\hbar$  and  $k_B$  momentarily so that Eq. (23) is phrased in terms of the ground-state energy of *oscillator-1* ( $E_g = \hbar\omega/2$ ) and the thermal energy scale ( $k_B T_{nl}$ ).

Now, let's take a moment to gain a clearer understanding of the result. The first condition describes the SDS of temperatures identified by us as allowing for exact solutions of the thermalization condition Eq. (17), as stated in the title of this subsection. This set is parametrized by two non-negative integers  $l$  and  $n$ . In term of the the average thermal energy  $U_\beta$  we can describe this set by rewriting Eq. (23) in the form

$$U_{\beta_{nl}} = E_g \left[ \frac{(2l+1)^2 + (2n+1)^2}{2(2l+1)(2n+1)} \right], \quad (27)$$

which is also manifestly symmetric under  $l \leftrightarrow n$ . Therefore, there is a sort *degeneracy* in that interchanging  $l \leftrightarrow n$  maps to the same temperature. As an example, consider  $\beta = \frac{k_B}{E_g} \log 2$ , for which we can identify  $(l, n)$  with either  $(0, 1)$  or  $(1, 0)$ . Consequently, there are two inequivalent sets of tunable parameters  $(\tilde{\omega}', \tilde{k}, \tilde{\tau})$ , namely,  $(1/\sqrt{3}, 4/3, \sqrt{3}/4)$  and  $(\sqrt{3}, -4/3, \sqrt{3}/4)$ , that give rise to the same inverse-temperature  $\beta = \frac{k_B}{E_g} \log 2$ . In general, under  $l \leftrightarrow n$ , the tunable parameters transform as  $\tilde{\omega}' \rightarrow 1/\tilde{\omega}'$ ,  $\tilde{k} \rightarrow -\tilde{k}$  and  $\tilde{\tau} \rightarrow \tilde{\tau}$ , as can easily be verified using Eq. (24), Eq. (25) and Eq. (26). In fact, at the level of the evolution of state of the full system, the transformation  $l \leftrightarrow n$ , effects  $b_+(t) \leftrightarrow b_-(t)$ , under which the reduced density matrix remains invariant. Another useful way of expressing the degeneracy is to give the expressions of  $\tilde{\omega}'$  and  $\tilde{k}$  as a function of the temperature.

$$\tilde{\omega}' = \begin{cases} \sqrt{\tanh\left(\frac{E_g}{2k_B T_{nl}}\right)} & ; \quad l < n \\ \sqrt{\coth\left(\frac{E_g}{2k_B T_{nl}}\right)} & ; \quad l > n \end{cases} \quad (28)$$

$$\tilde{k} = \begin{cases} \text{cosech}\left(\frac{E_g}{k_B T_{nl}}\right) & ; \quad l < n \\ -\text{cosech}\left(\frac{E_g}{k_B T_{nl}}\right) & ; \quad l > n \end{cases} \quad (29)$$

The envelope curves illustrating these relations are shown in Fig. 5. The plots are consistent with the intuitive expectation that achieving higher temperatures necessitates a more dramatic change in the oscillator frequency and a stronger coupling during the *active phase*.

We emphasize again that our protocol enables *exact* thermalization in a finite time. To quote the quickest case allowed by the SDS solutions, consider again  $\beta = \frac{k_B}{E_g} \log 2$ , where we can choose  $(l, n)$

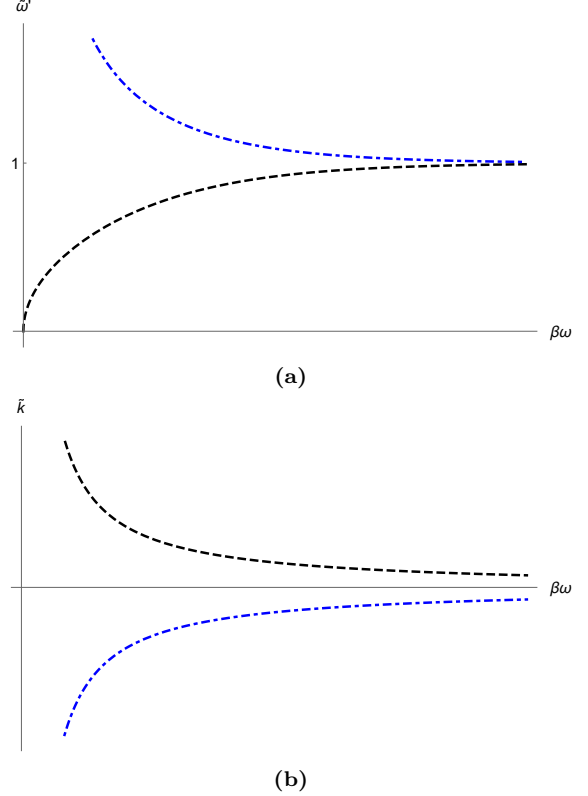


**FIG. 5:** The tunable parameters  $\tilde{\omega}'$  and  $\tilde{k}$  as a function of the SDS (inverse-)temperatures and as given in Eq. (28) and Eq. (29). The dashed and dot-dashed curves correspond to  $l < n$  and  $l > n$  cases, respectively. Note that these relations are valid only on the SDS  $T_{nl}$ .

to be either  $(1, 0)$  or  $(0, 1)$ . The time taken to thermalize, in dimensionless units, is then given by  $\tilde{\tau} = \sqrt{3}/4 \approx .433$ . In physical terms, this means that exact thermalization from the ground state occurs in about 43.3% of the oscillator's natural time-period.

The SDS temperatures, as such, do not cover all the possible values of temperature. However, it is worth emphasizing that this set is a countably dense subset of the set of all temperatures, which corresponds to the positive real line. This follows in view of Eq. (23) and the fact that odd-over-odd rational numbers form a countably dense subset of the real line. What this means is that for any given temperature  $T$  and an arbitrarily small error bar  $\delta T$ , one can always find a pair  $(l, n)$  such that

$$T - \delta T < T_{ln} < T + \delta T. \quad (30)$$

Since practically there is always an error bar or tolerance in an experimental context, by utilizing the SDS solutions, in principle, our protocol can, in fact,

be used to *approximate* thermalization to *arbitrary* values of temperature.

An important caveat in approximating a target temperature using the nearest value from the SDS is that achieving higher accuracy typically requires large  $l$  and  $n$ , which, from Eq. (26), entails longer thermalization times. This can be problematic when experimental constraints or resource limits impose an upper bound on  $\tau$ . However, faster thermalization may be achievable if we move beyond the SDS restriction.

As a preliminary step in this direction, let  $\vec{R}(\tilde{\omega}, \tilde{k}, \tilde{\tau})$  denote the components of the  $\vec{R}$ -vector for parameters  $\vec{P} = (P^1, P^2, P^3) \equiv (\tilde{\omega}, \tilde{k}, \tilde{\tau})$ . For a desired inverse temperature  $\beta = \beta_{nl} + \delta\beta$  near an SDS value, we can obtain an approximate perturbative correction to the control parameters by solving

$$\sum_{j=1}^3 \mathcal{M}_j^i \delta P^j = \delta\beta \frac{\partial R_{\beta_{nl}}^i}{\partial \beta}, \quad (31)$$

where

$$\mathcal{M}_j^i \equiv \frac{\partial R^i(\vec{P}_{nl})}{\partial P^j}, \quad (32)$$

and  $R_{\beta}^i$  are given in Eq. (8). For  $\det(\mathcal{M}) \neq 0$ , the first-order solution, with  $P^i = P_{nl}^i + \delta P^i$ , reads

$$\delta P^i = \delta\beta \left( \mathcal{M}^{-1} \right)_j^i \frac{\partial R_{\beta_{nl}}^j}{\partial \beta} + \mathcal{O}(\delta\beta^2). \quad (33)$$

Studying these linear perturbative solutions could shed light on the *local* structure of the thermalization condition's solution space. A complete characterization, however, requires a full numerical analysis of Eq. (17), which we leave for future work.

We now turn to analyzing the system's evolution toward the thermal state within our protocol.

### 1. Evolution to the thermal state

To visualize the time evolution of the density matrix as the system thermalizes under our protocol, we once again invoke the  $\vec{R}$ -space defined in Section II. As a first example, we revisit  $\beta = \frac{k_B}{E_g} \log 2$ , corresponding to the quickest case in the SDS. The evolution of *oscillator-1* from the ground state to the thermal state at this temperature is plotted in Fig. 6.

Next, to illustrate a case where the target temperature *does not* belong to the SDS, consider  $\beta =$

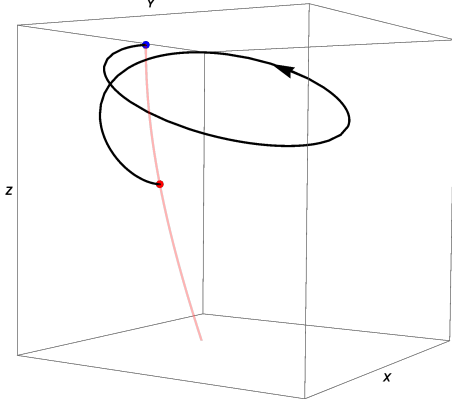


**FIG. 6:** Finite-time thermalization of oscillator 1 to the thermal state at  $\beta = \frac{k_B}{E_g} \log 2$ , starting from the ground state.

$\frac{k_B}{E_g} \pi$ . To a first approximation—accurate within about 1.16%—this temperature can be matched using the pair  $(l = 11, n = 12)$  or, equivalently,  $(l = 12, n = 11)$ , both yielding  $\beta \approx \frac{k_B}{E_g} \times 3.178$ . However, as we remarked earlier, one can always choose  $(n, l)$  values to match the desired temperature value of  $\beta = \frac{k_B}{E_g} \pi$  with arbitrary accuracy. To illustrate this, we have listed a few such choices in Tab. I, with the accuracy increasing as we move down the table. The corresponding evolution to the thermal state is presented in Fig. 7. As we pointed out earlier, the increased accuracy comes at the cost of increased time duration required for thermalization.

| $(l, n)$ | $E_g \beta_{nl} / k_B$ | $\delta\beta / \beta$ | $\tilde{\tau}$ |
|----------|------------------------|-----------------------|----------------|
| (12,11)  | 3.178                  | 1.16%                 | 5.99           |
| (24,22)  | 3.157                  | .49%                  | 11.74          |
| (36,33)  | 3.149                  | .26%                  | 17.48          |
| (48,44)  | 3.146                  | .15%                  | 23.23          |
| (60,55)  | 3.144                  | .08%                  | 28.97          |

**TABLE I:** List of SDS approximations to  $\beta = \pi k_B / E_g$ . As one moves down the list, the approximation error in temperature decreases by roughly a factor of two with each step. However, this improved accuracy comes at the cost of longer thermalization times, which in this example is scaling roughly inversely with the %-error in temperature.

Another way to study the thermalization process is by analyzing the time evolution of the average energy of the system—specifically, *oscillator-1*—as it approaches thermal equilibrium. The average en-

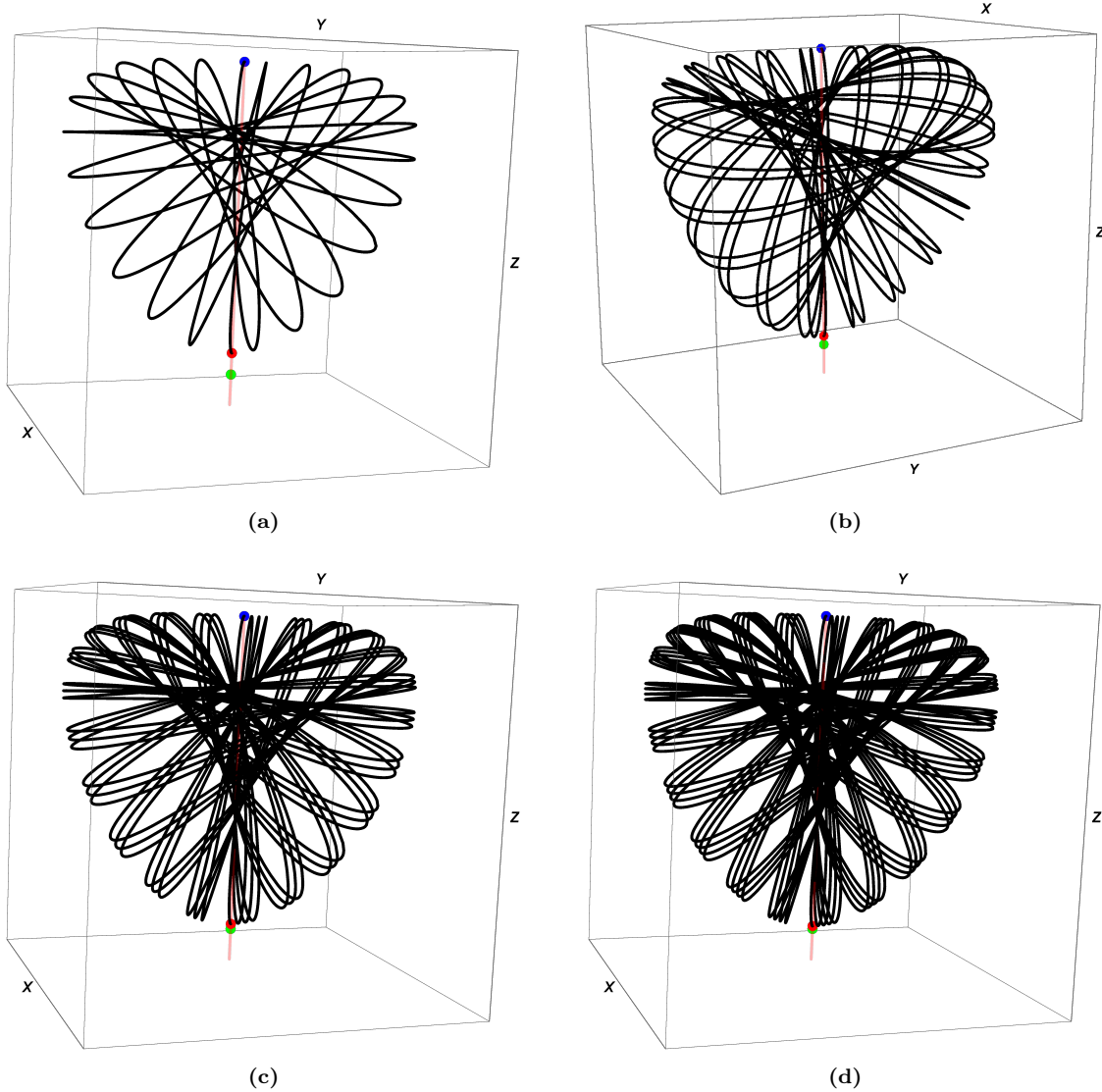


**FIG. 7:** Evolution toward the thermal state for various approximations to the target inverse temperature  $\beta = \frac{k_B}{E_g} \pi$ . The exact thermal state corresponding to this value is marked by a green dot, while the approximate thermal state is indicated by a red dot; both lie on the thermal curve. The associated  $(l, n)$  pairs are  $(12, 11)$ ,  $(24, 22)$ ,  $(36, 33)$ , and  $(48, 44)$  for panels (a), (b), (c), and (d), respectively.

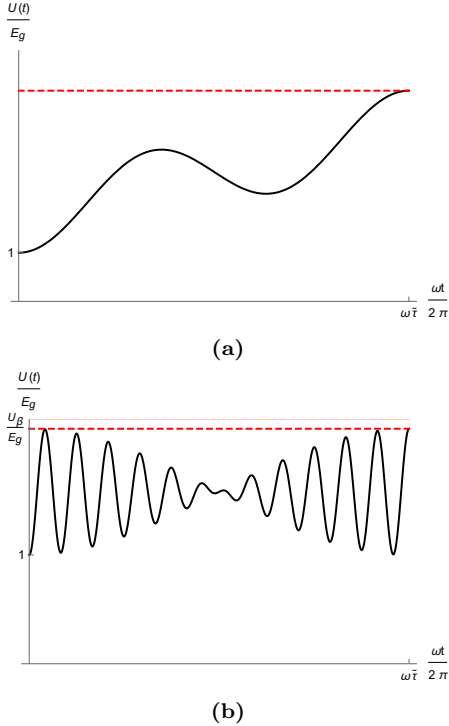


**FIG. 8:** Time evolution of  $U(t)$  shown as a solid black curve. The final thermal value is indicated by a dashed red line. (a)  $\beta = \frac{k_B}{E_g} \log 2$ , corresponding to  $(l, n) = (1, 0)$ , and (b)  $\beta \approx \frac{k_B}{E_g} \times 3.178$ , corresponding to  $(l, n) = (12, 11)$ . The thermal energy  $U_\beta$  for  $\beta = \frac{k_B}{E_g} \pi$  is also displayed in light red.

ergy  $U(t)$  is defined as

$$U(t) = \langle H_0 \rangle = \text{Tr} \left[ \rho^{(1)} H_0 \right], \quad (34)$$

$$H_0 = \frac{p_1^2}{2m} + \frac{1}{2}m\omega^2 x_1^2, \quad (35)$$

where  $H_0$  is the Hamiltonian of the first oscillator. A direct evaluation of the expectation value yields

$$U(t) = \frac{E_g}{2} \frac{(1 + X^2 + Y^2 - Z^2)}{(X + Z)}, \quad (36)$$

where the expression is written in terms of the components of  $\vec{R}$ . The evolution of the average energy toward the thermal value  $U_\beta$  is shown in Fig. 8 for two of the cases previously discussed:  $(l, n) = (1, 0)$  and  $(12, 11)$ . The observed oscillatory behavior is expected, given the structure of  $\rho^{(1)}$  in our setup.

This concludes our discussion on employing the proposed setup to thermalize a harmonic oscillator initially prepared in its ground state. Interestingly,

as a natural extension of the protocol, the same setup can also be used to either heat or cool *oscillator-1*. Before concluding, we now briefly outline how this can be achieved.

## B. Corollary: heating and cooling from quenching

We begin by recalling our earlier observation that the SDS arises when the normal mode frequencies of the *active phase* are commensurate. This condition ensures that the system's evolution is periodic. A remarkable consequence of this is that the same quench protocol that we introduced in the previous section can also be employed to *cool oscillator-1*—initially prepared in a thermal state corresponding to a temperature within the SDS—down to its ground state. In the energy-frequency diagram, this scenario corresponds to a reversal of the arrows shown in Fig. 4b.

As an illustrative example, consider the total system initially prepared in the purification of *oscillator-1*'s thermal state at inverse temperature  $\beta = \frac{k_B}{E_g} \log 2$ . Applying our protocol with parameters  $(\tilde{\omega}', \tilde{k}, \tilde{\tau}) = (1/\sqrt{3}, 4/3, \sqrt{3}/4)$  evolves the system into its ground state by the end of the *active phase*.

Taking this a step further, by applying two such quench protocols in sequence, one can effectively heat or cool the oscillator—that is, evolve it from an initial inverse temperature  $\beta_i$  to a final one  $\beta_f$ . This amounts to the following time dependence of the frequency and coupling:

$$\mathcal{K}(t) = \begin{cases} \omega^2 \tilde{k}_i & ; \quad 0 < t < \tau_i \\ \omega^2 \tilde{k}_f & ; \quad \tau_i < t < \tau_i + \tau_f \\ 0 & ; \quad \text{otherwise} \end{cases}, \quad (37)$$

$$\Omega(t) = \begin{cases} \omega \tilde{\omega}'_i & ; \quad 0 < t < \tau_i \\ \omega \tilde{\omega}'_f & ; \quad \tau_i < t < \tau_i + \tau_f \\ \omega & ; \quad \text{otherwise} \end{cases},$$

where the parameter sets  $(\tilde{\omega}'_i, \tilde{k}_i, \tilde{\tau}_i)$  and  $(\tilde{\omega}'_f, \tilde{k}_f, \tilde{\tau}_f)$  should be chosen according to Eq. (23)–Eq. (26), so as to correspond to the inverse temperatures  $\beta_i$  and  $\beta_f$ , respectively. A schematic of this process, along with the corresponding energy-frequency diagram, is shown in Fig. 9.

An interesting direction for future research is to examine the efficiency of the heating and cooling processes discussed above and to analyze their thermodynamic implications—for instance, by extending the single-oscillator treatment in [32] to our cou-

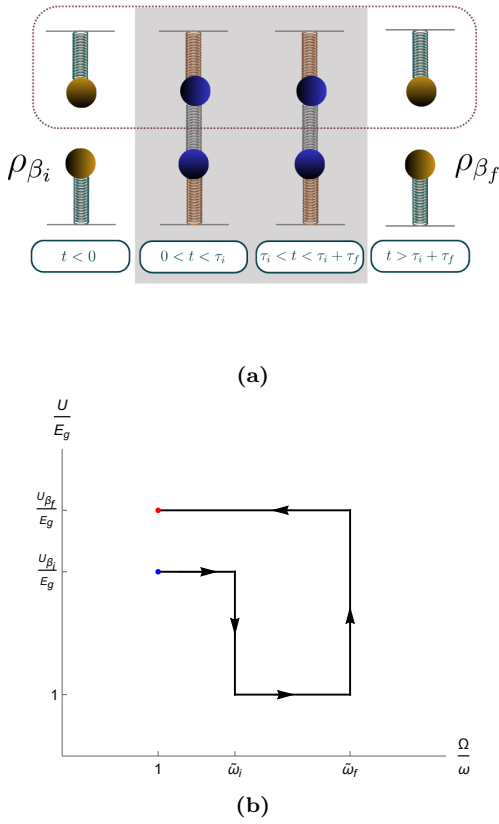


**FIG. 9:** (a) Adaptation of our protocol to enable either heating or cooling of *oscillator-1*. (b) The corresponding energy-frequency diagram, shown here for the case of heating.

pled system, or by exploring potential relevance to quantum thermal control [33]. While we have shown that the quench sequence can successfully achieve both heating and cooling, it is likely not the most efficient method within our setup. A promising avenue for future work is to optimize these processes in coupled oscillator systems through time-dependent control of the frequency and coupling parameters, employing techniques from optimal control theory [34].

## V. DISCUSSION

In this work, we have proposed and analyzed a simple, finite-time protocol for preparing a quantum harmonic oscillator in a thermal state starting from its ground state. By replacing a conventional macroscopic heat bath with a second oscillator and using a

short sequence of quenches in the oscillator frequencies and coupling strength, we have shown that exact thermalization can be engineered. The protocol relies on the Gaussian nature of the dynamics, which allows the reduced state of the target oscillator to be tracked compactly through the three-parameter vector  $\vec{R}(t)$ .

We demonstrated that the thermalization condition reduces to a set of three equations in the tunable parameters  $(\tilde{\omega}', \tilde{k}, \tilde{\tau})$ . While these equations are in general solvable numerically for arbitrary temperatures, we identified a *special discrete set* of temperatures for which the system admits exact, closed-form solutions. This set, labelled by two integers  $(l, n)$ , is countably dense in the positive real line of temperatures, implying that any target temperature can be approximated to arbitrary accuracy. The trade-off is that higher-accuracy approximations generally require longer evolution times during the *active phase*. We provided explicit formulae for the tuning parameters in this special set and examined representative examples, including the fastest-possible exact thermalization achievable in our scheme.

Beyond its conceptual simplicity, the protocol is broadly realizable: the required changes in coupling and frequency can be implemented in standard control operations in many experimental platforms, including, notably trapped ions[35]. Moreover, the scheme naturally connects to related quantum thermodynamic tasks such as refrigeration[36], state steering[37], or finite-time implementation of isochoric strokes in quantum heat engines[38, 39].

Several promising directions remain for future work. First, a comprehensive numerical survey of the thermalization condition’s solution space could uncover faster or more robust protocols beyond the current *special discrete set*. Second, incorporating realistic experimental constraints—such as finite quench rates, anharmonicity [40, 41], and decoherence—would provide a clearer picture of practical performance. Third, generalizing the approach to multimode or non-Gaussian regimes could yield richer thermalization dynamics and broaden its applicability. In the multimode setting, potential links to the quantum marginal problem [42] and possible implications for Hawking radiation [43, 44] would be especially compelling to explore.

In summary, our results show that finite-time, bath-free thermalization is not only theoretically possible but also analytically tractable in a large and experimentally relevant subset of cases.

## ACKNOWLEDGMENTS

KR is supported by the STFC Consolidated Grant ST/X000494/1 “Particle Theory at the Higgs Centre”. The authors thank Sreenath K Manikandan

and S Mahesh Chandran for several useful discussions. This work is part of MH’s master’s thesis; he sincerely thanks his internal guides, Shibi Thomas and Manesh Michael, for their comments and encouragement. MH also expresses gratitude to Lini Devassy and Anvy Moly Tom for their support and motivation.

---

[1] J. Goold, A. Riera, L. del Rio, M. Huber, and P. Skrzypczyk, “The role of quantum information in thermodynamics – a topical review,” *Journal of Physics A: Mathematical and Theoretical* **49** no. 14, (Feb., 2016) 143001.

[2] S. Deffner and S. Campbell, “Quantum thermodynamics: An introduction to the thermodynamics of quantum information,” 2019. <https://arxiv.org/abs/1907.01596>.

[3] J. Millen and A. Xuereb, “Perspective on quantum thermodynamics,” *New Journal of Physics* **18** no. 1, (2016) 011002.

[4] E. Witten, “Introduction to black hole thermodynamics,” *Eur. Phys. J. Plus* **140** no. 5, (2025) 430, [arXiv:2412.16795 \[hep-th\]](https://arxiv.org/abs/2412.16795).

[5] D. Harlow, “Jerusalem Lectures on Black Holes and Quantum Information,” *Rev. Mod. Phys.* **88** (2016) 015002, [arXiv:1409.1231 \[hep-th\]](https://arxiv.org/abs/1409.1231).

[6] S. Vinjanampathy and J. Anders, “Quantum thermodynamics,” *Contemporary Physics* **57** no. 4, (July, 2016) 545–579. <http://dx.doi.org/10.1080/00107514.2016.1201896>.

[7] N. M. Myers, O. Abah, and S. Deffner, “Quantum thermodynamic devices: From theoretical proposals to experimental reality,” *AVS Quantum Sci.* **4** no. 2, (2022) 027101, [arXiv:2201.01740 \[quant-ph\]](https://arxiv.org/abs/2201.01740).

[8] P. Hänggi and F. Marchesoni, “Artificial brownian motors: Controlling transport on the nanoscale,” *Reviews of Modern Physics* **81** no. 1, (Mar., 2009) 387–442. <http://dx.doi.org/10.1103/RevModPhys.81.387>.

[9] M. Horodecki and J. Oppenheim, “Fundamental limitations for quantum and nanoscale thermodynamics,” *Nature Communications* **4** no. 1, (June, 2013) . <http://dx.doi.org/10.1038/ncomms3059>.

[10] I. M. Georgescu, S. Ashhab, and F. Nori, “Quantum Simulation,” *Rev. Mod. Phys.* **86** (2014) 153, [arXiv:1308.6253 \[quant-ph\]](https://arxiv.org/abs/1308.6253).

[11] C.-F. Chen, M. J. Kastoryano, F. G. S. L. Brandão, and A. Gilyén, “Quantum Thermal State Preparation,” [arXiv:2303.18224 \[quant-ph\]](https://arxiv.org/abs/2303.18224).

[12] Z. Ding, Y. Zhan, J. Preskill, and L. Lin, “End-to-end efficient quantum thermal and ground state preparation made simple,” 2025. <https://arxiv.org/abs/2508.05703>.

[13] D. J. Wineland, C. Monroe, W. M. Itano, D. Leibfried, B. E. King, and D. M. Meekhof, “Experimental issues in coherent quantum-state manipulation of trapped atomic ions,” *J. Res. Natl. Inst. Stand. Tech.* **103** no. 3, (1998) 259, [arXiv:quant-ph/9710025](https://arxiv.org/abs/quant-ph/9710025).

[14] A. Wallraff, D. I. Schuster, A. Blais, L. Frunzio, R.-S. Huang, J. Majer, S. Kumar, S. M. Girvin, and R. J. Schoelkopf, “Strong coupling of a single photon to a superconducting qubit using circuit quantum electrodynamics,” *Nature* **431** no. 7005, (2004) 162–167. <https://www.nature.com/articles/nature02851>.

[15] M. Aspelmeyer, T. J. Kippenberg, and F. Marquardt, “Cavity Optomechanics,” *Rev. Mod. Phys.* **86** (2014) 1391, [arXiv:1303.0733 \[cond-mat.mes-hall\]](https://arxiv.org/abs/1303.0733).

[16] A. Bachtold, J. Moser, and M. I. Dykman, “Mesoscopic physics of nanomechanical systems,” *Rev. Mod. Phys.* **94** no. 4, (2022) 045005, [arXiv:2202.01819 \[cond-mat.mes-hall\]](https://arxiv.org/abs/2202.01819).

[17] R. Kosloff and Y. Rezek, “The quantum harmonic otto cycle,” *Entropy* **19** no. 4, (Mar., 2017) 136. <http://dx.doi.org/10.3390/e19040136>.

[18] S. Deffner, “Efficiency of harmonic quantum otto engines at maximal power,” *Entropy* **20** no. 11, (Nov., 2018) 875. <http://dx.doi.org/10.3390/e20110875>.

[19] A. Serafini, M. Lostaglio, S. Longden, U. Shackerley-Bennett, C.-Y. Hsieh, and G. Adesso, “Gaussian thermal operations and the limits of algorithmic cooling,” *Physical Review Letters* **124** no. 1, (Jan., 2020) . <http://dx.doi.org/10.1103/PhysRevLett.124.010602>.

[20] V. Singh and Ö. E. Müstecaplıoğlu, “Performance bounds of nonadiabatic quantum harmonic otto engine and refrigerator under a squeezed thermal reservoir,” *Physical Review E* **102** no. 6, (Dec., 2020) . <http://dx.doi.org/10.1103/PhysRevE.102.062123>.

[21] G. Benenti and G. Strini, “Dynamical casimir effect and minimal temperature in quantum thermodynamics,” *Phys. Rev. A* **91** (Feb, 2015) 020502. <https://link.aps.org/doi/10.1103/PhysRevA.91.020502>.

[22] S. Suomela, A. Kutvonen, and T. Ala-Nissila, “Quantum jump model for a system with a

finite-size environment,” *Phys. Rev. E* **93** (Jun, 2016) 062106. <https://link.aps.org/doi/10.1103/PhysRevE.93.062106>.

[23] B. Reid, S. Pigeon, M. Antezza, and G. De Chiara, “A self-contained quantum harmonic engine,” *EPL (Europhysics Letters)* **120** no. 6, (Dec., 2017) 60006. <http://dx.doi.org/10.1209/0295-5075/120/60006>.

[24] M. N. Bera, A. Riera, M. Lewenstein, Z. B. Khanian, and A. Winter, “Thermodynamics as a consequence of information conservation,” *Quantum* **3** (Feb., 2019) 121. <http://dx.doi.org/10.22331/q-2019-02-14-121>.

[25] E. Torrontegui, S. Ibáñez, S. Martínez-Garaot, M. Modugno, A. del Campo, D. Guéry-Odelin, A. Ruschhaupt, X. Chen, and J. G. Muga, “Shortcuts to Adiabaticity,” *Adv. At. Mol. Opt. Phys.* **62** (2013) 117–169, [arXiv:1212.6343](https://arxiv.org/abs/1212.6343) [quant-ph].

[26] A. del Campo and K. Kim, “Focus on shortcuts to adiabaticity,” *New Journal of Physics* **21** no. 5, (May, 2019) 050201. <http://dx.doi.org/10.1088/1367-2630/ab1437>.

[27] V. P. Ermakov, “Second order differential equations: conditions of complete integrability,” *Univ. Izv. Kiev* **20** no. 9, (1880) 1.

[28] H. R. Lewis Jr, “Classical and quantum systems with time-dependent harmonic-oscillator-type hamiltonians,” *Physical Review Letters* **18** no. 13, (1967) 510.

[29] H. R. Lewis Jr, “Class of exact invariants for classical and quantum time-dependent harmonic oscillators,” *Journal of Mathematical Physics* **9** no. 11, (1968) 1976–1986.

[30] C. Monroe, D. Meekhof, B. King, S. R. Jefferts, W. M. Itano, D. J. Wineland, and P. Gould, “Resolved-sideband raman cooling of a bound atom to the 3d zero-point energy,” *Physical review letters* **75** no. 22, (1995) 4011.

[31] D. Meekhof, C. Monroe, B. King, W. M. Itano, and D. J. Wineland, “Generation of nonclassical motional states of a trapped atom,” *Physical review letters* **76** no. 11, (1996) 1796.

[32] S. Deffner and E. Lutz, “Nonequilibrium work distribution of a quantum harmonic oscillator,” *Physical Review E—Statistical, Nonlinear, and Soft Matter Physics* **77** no. 2, (2008) 021128.

[33] E. Jussieu, S. K. Manikandan, B. Bhandari, and A. N. Jordan, “Thermal control across a chain of electronic nanocavities,” *Physical Review B* **104** no. 4, (July, 2021) . <http://dx.doi.org/10.1103/PhysRevB.104.045414>.

[34] D. E. Kirk, *Optimal Control Theory: An Introduction*. Courier Corporation, Mineola, NY, 2004. [https://books.google.com/books/about/Optimal\\_Control\\_Theory.html?id=fCh2SATWIdwC](https://books.google.com/books/about/Optimal_Control_Theory.html?id=fCh2SATWIdwC).

[35] C. Ospelkaus, U. Warring, Y. Colombe, K. R. Brown, J. M. Amini, D. Leibfried, and D. J. Wineland, “Microwave quantum logic gates for trapped ions,” *Nature* **476** no. 7359, (Aug., 2011) 181–184. <http://dx.doi.org/10.1038/nature10290>.

[36] N. Freitas and J. P. Paz, “Cooling a quantum oscillator: A useful analogy to understand laser cooling as a thermodynamical process,” *Phys. Rev. A* **97** (Mar, 2018) 032104. <https://link.aps.org/doi/10.1103/PhysRevA.97.032104>.

[37] D. Kienzler, H.-Y. Lo, B. Keitch, L. de Clercq, F. Leupold, F. Lindenfelser, M. Marinelli, V. Negnevitsky, and J. P. Home, “Quantum harmonic oscillator state synthesis by reservoir engineering,” *Science* **347** no. 6217, (Jan., 2015) 53–56. <http://dx.doi.org/10.1126/science.1261033>.

[38] J. Roßnagel, O. Abah, F. Schmidt-Kaler, K. Singer, and E. Lutz, “Nanoscale heat engine beyond the carnot limit,” *Physical Review Letters* **112** no. 3, (Jan., 2014) . <http://dx.doi.org/10.1103/PhysRevLett.112.030602>.

[39] J. Roßnagel, S. T. Dawkins, K. N. Tolazzi, O. Abah, E. Lutz, F. Schmidt-Kaler, and K. Singer, “A single-atom heat engine,” *Science* **352** no. 6283, (Apr., 2016) 325–329. <http://dx.doi.org/10.1126/science.aad6320>.

[40] S. Deffner, O. Abah, and E. Lutz, “Quantum work statistics of linear and nonlinear parametric oscillators,” *Chemical Physics* **375** no. 2-3, (2010) 200–208.

[41] Y. Zheng and D. Poletti, “Work and efficiency of quantum otto cycles in power-law trapping potentials,” *Physical Review E* **90** no. 1, (2014) 012145.

[42] A. A. Klyachko, “Quantum marginal problem and n-representability,” *Journal of Physics: Conference Series* **36** (Apr., 2006) 72–86. <http://dx.doi.org/10.1088/1742-6596/36/1/014>.

[43] E. Aurell, L. Hackl, P. Horodecki, R. H. Jonsson, and M. Kieburg, “Random Pure Gaussian States and Hawking Radiation,” *Phys. Rev. Lett.* **133** no. 6, (2024) 060202, [arXiv:2311.10562](https://arxiv.org/abs/2311.10562) [gr-qc].

[44] E. Aurell, L. Hackl, and M. Kieburg, “Average entanglement entropy of a small subsystem in a constrained pure Gaussian state ensemble,” [arXiv:2505.03696](https://arxiv.org/abs/2505.03696) [quant-ph].